

Article

Effect of the Rehydration Method on the Physical–Mechanical Properties of CO₂-Cured Magnesium-Based Fiber Cement Boards

Adriano G. S. Azevedo ^{1,*}, Juan Camilo Adrada Molano ¹, Igor Parente ¹, Taís O. G. Freitas ¹, Aires Camões ², Paulina Faria ³ and Holmer Savastano, Jr. ¹

¹ Department of Biosystems Engineering, University of São Paulo, Pirassununga 13635-900, Brazil; camiloadrada@usp.br (J.C.A.M.); igorparente@usp.br (I.P.); taisfreitas@usp.br (T.O.G.F.); holmersj@usp.br (H.S.J.)

² CTAC—Center for Territory, Environment and Construction, University of Minho, 4800-058 Guimarães, Portugal; aires@civil.uminho.pt

³ CERIS, Department of Civil Engineering, NOVA School of Science and Technology, NOVA University Lisbon, 2829-516 Caparica, Portugal; mpr@fct.unl.pt

* Correspondence: adrianogalvao@usp.br

Abstract: This article analyzes the effect of the rehydration method on the physical–mechanical properties of accelerated carbonation-cured magnesium-based fiber cement boards. The rehydration process of the boards was analyzed in conjunction with the analysis of the pre-curing time before accelerated carbonation (24, 48, and 72 h before carbonation), resulting in eight different curing parameters used in this investigation. The physical–mechanical performance and microstructural characteristics of magnesium oxysulfate boards before and after carbonation were investigated by water absorption, apparent porosity, and bulk density using the four-point bending test, X-ray diffraction, thermogravimetric analysis, and scanning electron microscopy. According to the results, the accelerated carbonation process improved the mechanical properties of the boards. The samples that carbonated after 48 h showed a higher modulus of rupture. The rehydration process of the composites before carbonation led to enhancements in the pre-cured boards for 48 and 72 h, demonstrating that carbonation occurred more effectively after water rehydration. The mechanical improvements were associated with the formation of hydration products, which preferentially formed in the pores and voids of the fiber cement matrix. These carbonation products altered the physical properties of the composites, increasing the density of the boards and reducing the void volume. The decomposition of the formed carbonates was confirmed by thermogravimetric analysis, which indicated that the rehydration process favored the carbonation of the composites.

Keywords: MOS cement; rehydration method; carbonation; fiber cement boards; civil construction



Citation: Azevedo, A.G.S.; Molano, J.C.A.; Parente, I.; Freitas, T.O.G.; Camões, A.; Faria, P.; Savastano, H., Jr. Effect of the Rehydration Method on the Physical–Mechanical Properties of CO₂-Cured Magnesium-Based Fiber Cement Boards. *CivilEng* **2024**, *5*, 247–264. <https://doi.org/10.3390/civileng5010013>

Academic Editors: Akanshu Sharma and Angelo Luongo

Received: 29 October 2023

Revised: 19 January 2024

Accepted: 13 March 2024

Published: 16 March 2024



Copyright: © 2024 by the authors. Licensee MDPI, Basel, Switzerland. This article is an open access article distributed under the terms and conditions of the Creative Commons Attribution (CC BY) license (<https://creativecommons.org/licenses/by/4.0/>).

1. Introduction

Despite non-conclusive predictions regarding the forthcoming impacts of climate change, a direct relationship exists between global warming and the heightened concentration of greenhouse gases in the atmosphere [1]. The carbon dioxide (CO₂) emissions resulting from the combustion of fossil fuels are of particular concern due to the greenhouse effect of this gas. An important source of CO₂ emissions is the production of ordinary Portland cement (OPC) [2]. OPC is the most used cement in the construction industry, and the manufacturing process involves high CO₂ emissions, primarily from the decomposition of carbonates, such as limestone, and the burning of coal at high temperatures, around 1500 °C [3]. The emissions generated in cement production consist of 5 to 7% of total global CO₂ emissions [4,5], making it necessary to develop alternative cementitious materials to replace the conventional ones.

Magnesium oxide (MgO)-based cements have been identified as promising alternative binders due to their carbon sequestration potential and lower energy consumption

compared with OPC [6–8]. MgO production mainly comes from the calcination of magnesite (MgCO_3) [9]. Generally, MgO is categorized into the following different grades [10]: light-burned MgO (LBM) or caustic-calcined MgO (calcined at 700–1000 °C), which has the highest reactivity and specific surface area; hard-burned MgO (calcined at 1000–1500 °C), with lower reactivity and specific surface area compared with LBM; dead-burned or periclase MgO (calcined at 1400–2000 °C), with the lowest specific surface area, making it almost non-reactive; and fused magnesia (calcined at $T > 2800$ °C) with the lowest reactivity [11,12]. Also, MgO can be obtained by the wet route from brine or seawater solutions containing magnesium; in this wet route, brucite ($\text{Mg}(\text{OH})_2$) is the MgO precursor, which has no chemically combined CO_2 [13].

Magnesium oxysulfate (MOS) cement is a type of non-hydraulic binder prepared from the reaction between magnesium oxide (MgO) and an aqueous solution of magnesium sulfate (MgSO_4) [12,14,15]. It bears several advantages, including good fire resistance, lightweight properties, low alkalinity, and low-energy consumption, with the production of lightweight panels being its primary application [16–18]. In general, four oxysulfate phases are found at temperatures between 30 and 120 °C: (I) $3\text{Mg}(\text{OH})_2\text{-MgSO}_4\text{-}8\text{H}_2\text{O}$ (3-1-8 phase); (II) $5\text{Mg}(\text{OH})_2\text{-MgSO}_4\text{-}3\text{H}_2\text{O}$ (5-1-3 or 5-1-2 phase); (III) $\text{Mg}(\text{OH})_2\text{-MgSO}_4\text{-}5\text{H}_2\text{O}$ (1-1-5 phase); and (IV) $\text{Mg}(\text{OH})_2\text{-}2\text{MgSO}_4\text{-}3\text{H}_2\text{O}$ (1-2-3 phase) [19].

MOS cement is susceptible to carbonation throughout its curing process and service life. This phenomenon involves the reaction of magnesium hydroxide with CO_2 , forming hydrated magnesium carbonate (HMC). The conversion process can be divided into the following three essential stages: initially, MgO reacts with water to form $\text{Mg}(\text{OH})_2$; then, CO_2 dissolves in the water, giving rise to carbonic acid; finally, the reaction between magnesium hydroxide and carbonate ions takes place, culminating in the formation of HMC, which significantly improves mechanical strength [20]. In addition, construction composites made with this type of cement can have a high proportion of cellulose fibers due to the reduced alkalinity of the matrix [21], such as eucalyptus fibers, leading to lower total CO_2 emissions when compared with OPC-based building materials.

In carbonation reactions, the primary carbonates formed include the formation of magnesite from MgO by absorbing CO_2 ($\text{MgO} + \text{CO}_2 \rightarrow \text{MgCO}_3$) or incorporating H_2O to form needle-like nesquehonite ($\text{MgCO}_3\cdot 3\text{H}_2\text{O}$), acicular artinite ($\text{MgCO}_3\cdot \text{Mg}(\text{OH})_2\cdot 3\text{H}_2\text{O}$), and disk-like hydro-magnesite ($4\text{MgCO}_3\cdot \text{Mg}(\text{OH})_2\cdot 4\text{H}_2\text{O}$) [22]. The hydrates formed, depending on the curing conditions, lead to a gain in mechanical strength due to their inherent resistance and their capacity to bind aggregate particles [9].

Sun Qi et al. [23] found that carbonation not only enhances the toughness of MOS cement to some extent but also leads to a further reduction in porosity. Ba et al. [16] demonstrated a decrease in the alkalinity and porosity of MOS cement. These findings may enhance the durability of cellulose fibers within this type of matrix. According to Qiyang Li et al. [24], incorporating CO_2 capture during cement curing significantly enhances resistance to wetting–drying cycles. The results suggest that CO_2 neutralizes magnesium hydroxide and some basic phases of magnesium oxysulfate within MOS cement, resulting in the formation of magnesium carbonate phases, thereby refining pore structures and increasing the overall strength.

Some studies focus on the influence of rehydration on the properties of OPC materials [22,23]. Nevertheless, the impact of rehydration on the carbonation of MOS cement remains a relatively underexplored subject. This work analyzed the influence of the rehydration method applied to magnesium oxysulfate cement boards before carbonation curing. The physical–mechanical performance and microstructural characteristics of MOS boards before and after carbonation were investigated by water absorption (WA), apparent porosity (AP), and bulk density (BD) using the four-point bending test, X-ray diffraction (XRD), thermogravimetric analysis (TGA), and scanning electron microscopy (SEM).

2. Materials and Methods

2.1. Materials

The MOS-based fiber cement boards were produced with a mixture of magnesium oxide powder (MgO), magnesium sulfate heptahydrate ($\text{MgSO}_4 \cdot 7\text{H}_2\text{O}$), dolomitic limestone and citric acid, and reinforced with unbleached *Eucalyptus* cellulose fiber.

The MgO, obtained by the controlled calcination of magnesite ($1050\text{ }^\circ\text{C}$), was purchased from RHI-Magnesita S.A., (Brumado, BA, Brazil). It has a specific gravity of 3.45 g/cm^3 and a surface area of $26.71\text{ m}^2/\text{g}$. Figure 1 shows that the particle size of MgO presents values of D10, D50, and D90 close to 2.1, 8.8, and $40.0\text{ }\mu\text{m}$, respectively.

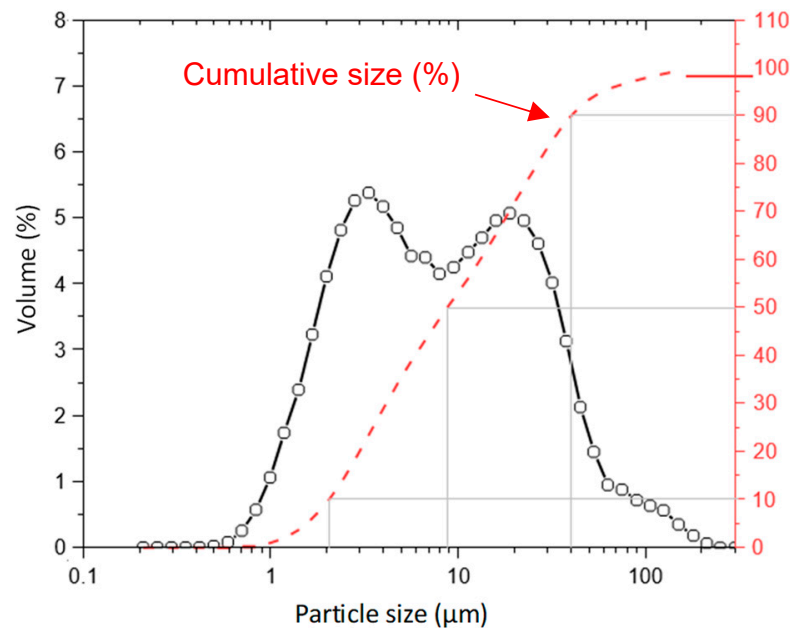


Figure 1. Particle size distribution of MgO used to produce the MOS cement boards.

Magnesium sulfate heptahydrate (commercial-grade Epsom salt, $\text{MgSO}_4 \cdot 7\text{H}_2\text{O}$) was produced with 99.83% purity. Table 1 and Figure 2 show the chemical composition and the X-ray diffractogram pattern of the MgO used, respectively. Figure 2 shows different diffraction peaks related to periclase (MgO), with the peak close to $42^\circ 2\theta$ having the highest intensity, as shown in ICDD No. 00-0004-0829. The chemical composition of MgO shows a high concentration of MgO, as suggested by the manufacturer. In contrast, dolomitic limestone has a high content of CaO in its composition and exhibits a loss of ignition of approximately 40%, which is attributed to the presence of carbonates in the material. Dolomite limestone used as a filler in the fiber cement boards has a 2.79 g/cm^3 density. Citric acid of analytical purity was used in the mixture at a proportion of 0.50% of the mass of MgO. Unbleached *Eucalyptus* pulp was used as lignocellulosic reinforcement in the fiber cement boards produced. The fiber was processed in water (kept in water immersion for 48 h) and then disintegrated using a cellulosic pulp mixer, Tedemix MRF31450 (São Paulo, SP, Brazil). Morphological characterization (Figures 3 and 4) was carried out using an adapted TAPPI T271 standard [25]. The chemical composition of cellulosic pulp was determined following the procedure by Van Soest [26]. The authors analyzed the vegetable fiber components, considering the chemical compounds in the cell (lipids, fats, etc.) and cell wall (cellulose, hemicellulose, lignin, and insoluble protein). Table 2 shows the chemical composition of unbleached *Eucalyptus* pulp.

Table 1. Chemical composition and loss of ignition (LOI) of MgO and dolomitic limestone used in the MOS-based board formulation.

Compound	Dolomitic Limestone (wt%)	MgO(wt%)
MgO	7.6	97.4
Al ₂ O ₃	1.03	<0.10
SiO ₂	3.99	0.1
P ₂ O ₅	0.05	–
SO ₃	0.13	–
Cl	0.01	–
K ₂ O	0.22	<0.10
Na ₂ O	–	<0.10
CaO	43.9	0.81
TiO ₂	0.06	–
MnO	0.09	–
Fe ₂ O ₃	0.42	–
ZnO	<0.01	–
Rb ₂ O	<0.02	–
SrO	<0.03	–
LOI	42.4	1.6

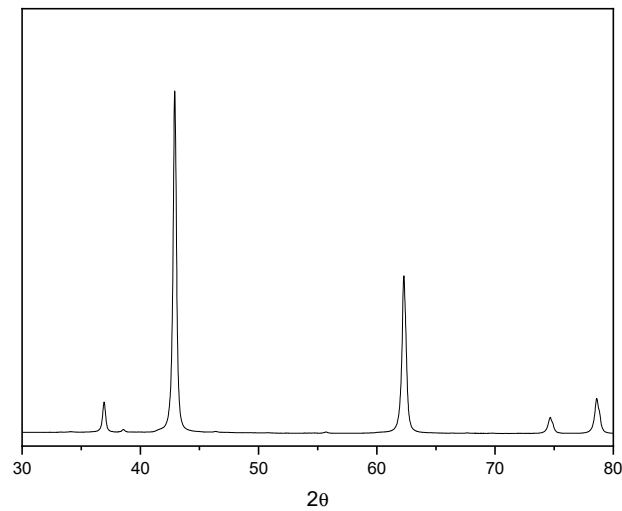


Figure 2. X-ray diffraction of MgO used to produce the MOS cement boards.

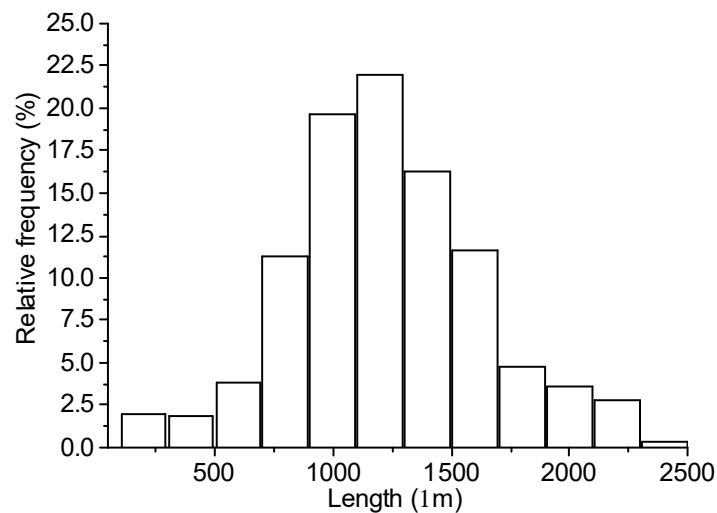


Figure 3. Histogram of the length distribution of pulp reinforcement.

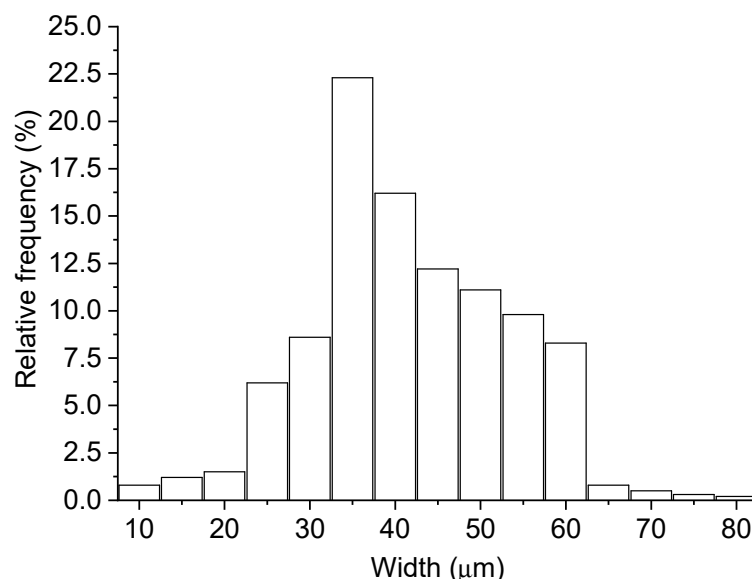


Figure 4. Histogram of the width distribution of pulp reinforcement.

Table 2. Chemical composition of unbleached *Eucalyptus* fiber used as reinforcement in the fiber cement.

Type of Fiber	Chemical Composition (%)			
	Cellulose	Hemicellulose	Lignin	Others
<i>Eucalyptus</i> (unbleached)	82.55	8.39	1.73	7.33

2.2. Methods

2.2.1. Sample Preparation

The fiber-cement boards were prepared in the laboratory by the slurry vacuum de-watering technique (an adapted industrial Hatschek process), as described by Savastano et al. (2000) [27]. The cellulose pulp was initially dispersed in a mixture of distilled water and $MgSO_4$ solution with a 25% concentration and 0.50% of citric acid at 3000 rpm for 5 min. Subsequently, MgO, in a $MgO:MgSO_4$ molar ratio of 10, and dolomitic limestone, constituting 20% of the MgO by mass (previously homogenized), were added, and the mixture was stirred for another 3 min. The slurry was transferred and subjected to a vacuum until the initial excess water was removed, leading to the formation of a solid surface. The wet boards were transferred to a pressure machine and compacted for 5 min at 3.2 MPa. The boards were kept at a controlled temperature and relative humidity, at 25 °C and 60%, respectively, until the beginning of the carbonation process (Figure 5A).

2.2.2. Accelerated Carbonation Process

To evaluate the effect of carbonation at the early ages of curing, the samples were kept in a hermetically sealed environment before being cured in a CO_2 -rich atmosphere. All samples were exposed to a concentrated CO_2 environment of 20% CO_2 and 60% relative humidity (RH) at 40 °C for 6 h to accelerate the carbonation process. The parameters were adjusted based on previous work on the carbonation of MOS cement [6]. The boards were carbonated after 24, 48, and 72 h of production and were named Carb24, Carb48, and Carb72, respectively. The samples cured without carbonation were named Ref. A climatic chamber with the control of temperature, RH, and CO_2 concentration, Espec brand, model EPL-4H (Aurora, CO, USA), was used, as shown in Figure 5C. Table 3 shows the different samples produced by accelerated carbonation.

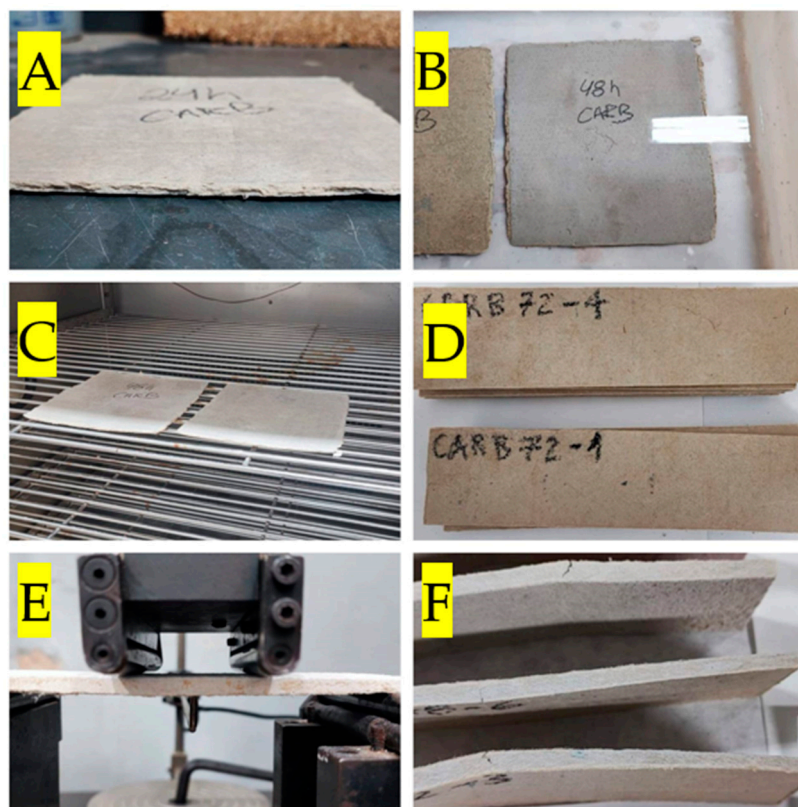


Figure 5. Fiber cement board samples production and characterization: (A) pre-cured board (Carb24); (B) boards during rehydration process (Carb48-RE); (C) boards inside the carbonation chamber; (D) composite specimens (160 × 40 × 5 mm); (E) 4-point-bending flexural test, and (F) boards after mechanical characterization.

Table 3. Different boards produced by rehydration and accelerated carbonation processes.

Sample	Boards Produced
Ref	Without rehydration and carbonation
Ref-RE	Rehydrated-uncarbonated boards
Carb24	Carbonated after 24 h without rehydration
Carb48	Carbonated after 48 h without rehydration
Carb72	Carbonated after 72 h without rehydration
Carb24-RE	Carbonated after 24 h with rehydration
Carb48-RE	Carbonated after 48 h with rehydration
Carb72-RE	Carbonated after 72 h with rehydration

In preparation for subsequent carbonation, fiber cement boards underwent an essential rehydration stage with water immersion. This preliminary step aimed to reinstate moisture and create optimal conditions for effective carbonation. Table 3 shows that the boards Carb24-RE, Carb48-RE, and Carb72-RE were submerged in water for 5 min to ensure thorough hydration, followed by the draining of excess water (Figure 5B). This process created an ideal environment for the subsequent carbonation phase. The rehydrated boards transitioned into the carbonation process, highlighting the efficacy of pre-immersion hydration in optimizing the final properties of the fiber cement boards.

2.2.3. Board Characterization

The physical, mechanical, and microstructural characterization of the boards was performed 7 days after molding. The test samples were cut to dimensions of 160 × 40 × 5 mm (Figure 5D). A total of eight test specimens were used for the mechanical and physical analysis of the boards produced under varying conditions.

ASTM-C948-81 [28] was used to determine the physical properties. Water absorption (WA), apparent porosity (AP), and bulk density (BD) were the examined parameters.

A four-point bending test was performed on the boards to evaluate their mechanical properties, as shown in Figure 5E [28]. The test was conducted using an EMIC (São José dos Pinhais, PR, Brazil) DL30000 universal mechanical testing machine equipped with a 5 kN load cell and a deflectometer to detect the displacement in the center of the specimen. A span of 135 mm was used between the bottom supports, and 45 mm was used between the top supports, along with a load speed of 5 mm/min. The deflection during the bending test was collected by the deflectometer positioned in the middle span on the underside of the specimen. The deflectometer used was an EMIC brand with a maximum deformation of 30 mm and 0.0001 mm accuracy. The modulus of rupture (MOR), the limit of proportionality (LOP), the modulus of elasticity (MOE), and specific energy (SE) were determined using the methodology employed by Savastano Junior et al. (2000) and RILEM [27,29].

To identify phase evolution, X-ray diffraction (XRD) and scanning electron microscopy (SEM) were carried out on samples extracted before and after each different carbonation condition (Figure 5F). The X-ray powder diffraction (XRD) patterns of the fiber cement boards were collected using a Horiba LA-60 diffractometer using $\text{CuK}\alpha$ radiation generated at a voltage of 40 kV and a tube current of 30 mA, with scan angles ranging from 10 to 70° at a rate of 2°/min. The morphological analyses were performed using a Philips XL-30 FEG (Field Emission Gun) microscope.

Samples were prepared following the same procedure used in X-ray diffraction. Thermogravimetry (TGA) was used to measure the changes in mass within the fiber cement samples due to temperature. TGA analysis was employed to evaluate the constituents generated during the MOS cement production and assess the carbonation in the formation of new products. The analysis was conducted using a TA Instruments (New Castle, DE, UK) SDT 600 model, with a heating rate of 10 °C/min, reaching 1000 °C, and a nitrogen flow rate of 40 mL/min.

3. Results

3.1. Mechanical Properties

Table 4 shows the results of flexural tests conducted on carbonated cementitious composites under varying conditions and the reference samples. The accelerated carbonation process applied to the composites evidently induced alterations in the mechanical properties of the boards. The carbonation process, without prior rehydration, notably enhanced the properties of samples cured for 48 h. Carb48 boards exhibited an average increase in MOR values of approximately 14.7%, 25.34%, and 32.4% when compared with the Ref, Carb24, and Carb72 samples, respectively.

Table 4. Mechanical proprieties of rehydrated and non-rehydrated-carbonated MOS-based fiber cement composites.

Sample	MOR	LOP	MOE	SE
	(MPa)	(MPa)	(GPa)	(KJ/m ²)
Ref	15.16 ± 0.63	12.40 ± 1.95	9.89 ± 1.24	3.44 ± 0.48
Carb24	13.79 ± 1.16	10.23 ± 1.47	9.90 ± 1.60	2.71 ± 0.33
Carb48	18.47 ± 0.95	14.66 ± 0.90	10.52 ± 1.37	2.93 ± 0.1
Carb72	12.48 ± 1.22	10.79 ± 2.88	8.26 ± 1.16	2.63 ± 0.37
Ref-RE	13.81 ± 1.63	8.75 ± 0.29	9.48 ± 0.34	4.41 ± 1.11
Carb24-RE	16.16 ± 0.97	12.03 ± 1.65	13.44 ± 1.69	3.60 ± 1.63
Carb48-RE	18.51 ± 1.18	12.73 ± 1.02	14.83 ± 1.48	3.28 ± 0.31
Carb72-RE	19.31 ± 0.70	12.39 ± 1.22	13.57 ± 0.25	4.08 ± 0.62

The carbonation process is responsible for generating new carbonate products. These reactions occur between the CO₂ present in the carbonation chamber and the alkali species

within the cementitious matrix used as the base in composite production. As described by Meng et al. [6], the reactions associated with the formation of carbonates in MgO-based cement matrices are presented in Equations (1)–(3).

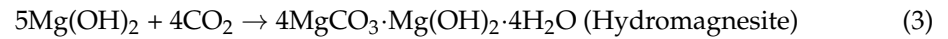
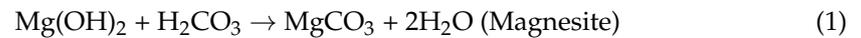


Table 4 shows that the formation of carbonates preferentially occurs in the voids and pores within the cementitious matrix, which is associated with increased stiffness and, consequently, the mean MOE values of the composites. The changes in mechanical properties observed in boards cured for different periods may be linked to the formation of alkali species that are consumed during carbonation in a CO₂-rich atmosphere. The longer pre-carbonation curing period may be associated with the hydration kinetics of MgO particles in the formation of brucite (Mg(OH)₂). Samples carbonated after 24 h exhibited lower mechanical performance than samples carbonated after 48 h. This may be related to the increased availability of alkali species after 48 h of MgO particle hydration with available water in the system. In contrast, after 72 h, the carbonation process led to a decrease in the mean MOR values, representing a decrease of approximately 17%. The carbonation process reduced the mean SE values of the produced composites. This is associated with the increased stiffness of the boards and a reduction in the total voids within the cementitious matrix.

Figures 6 and 7 show the typical tension–deflection curves of the non-rehydrated and rehydrated MOS-based composites.

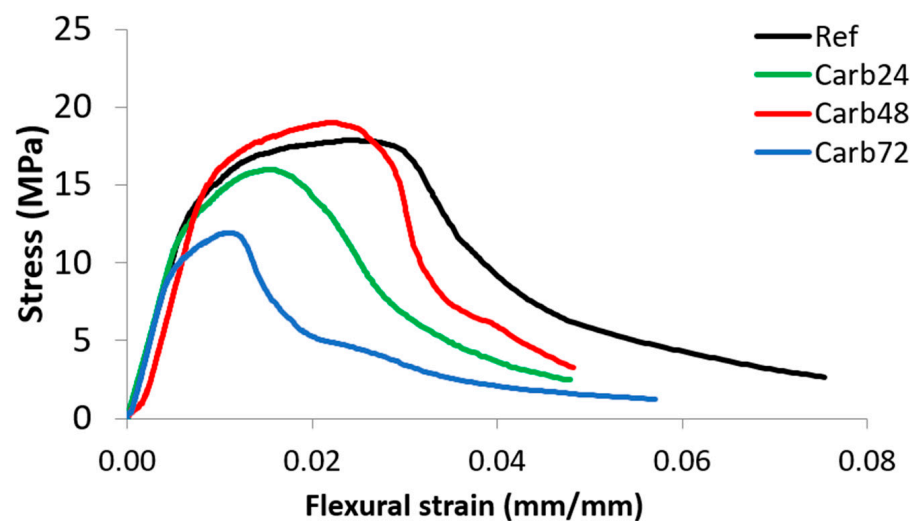


Figure 6. Tension–deflection curves of the non-rehydrated MOS-based composites.

Comparing Figures 6 and 7, the rehydration process of the samples before curing in a CO₂-rich atmosphere increased the mechanical strength of the materials. The reference composites showed lower gains in mechanical strength when compared with the non-rehydrated materials. This was associated with the increased formation of brucite in the materials after rehydration, which promoted the formation of microcracks during the expansion of Mg(OH)₂ crystals, leading to a decrease in the mechanical strength of the boards. Composites rehydrated and carbonated after 48 and 72 h exhibited the highest gains in mechanical strength among the boards studied. This was associated with the increased formation of alkali species at 48 and 72 h after board production and immersion in water before carbonation curing.

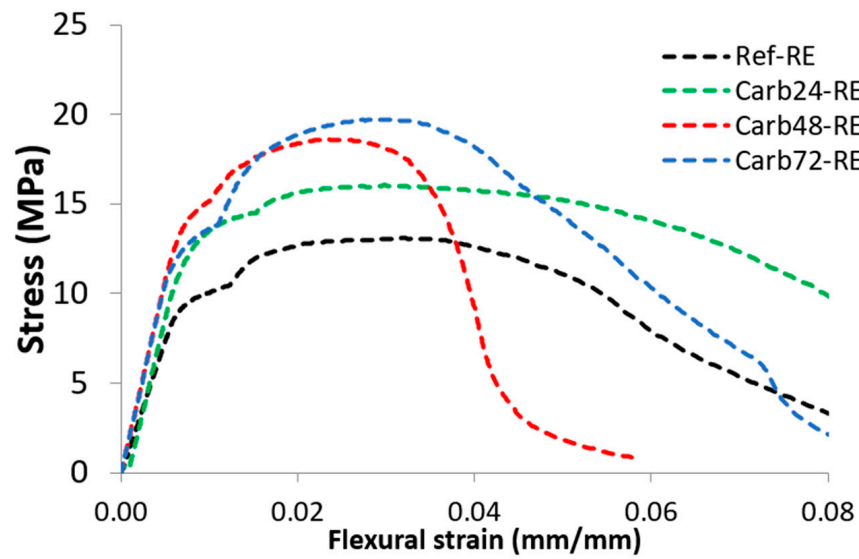


Figure 7. Tension–deflection curves of the rehydrated MOS-based composites.

Figures 8 and 9 show the effect of accelerated carbonation on the properties of rehydrated and non-rehydrated fiber cement boards. The carbonation process led to a trend of decreasing the mean values of the apparent void volume in the produced composites. However, the alteration of the pre-carbonation period modified the MOR values of the boards. Composites carbonated after 48 h (Carb28) showed a mean void volume and MOR values close to 28% and 18.5 MPa, respectively. The rehydration of the boards reduced void values to around 23.5% and maintained the mean MOR values at 18.5 MPa.

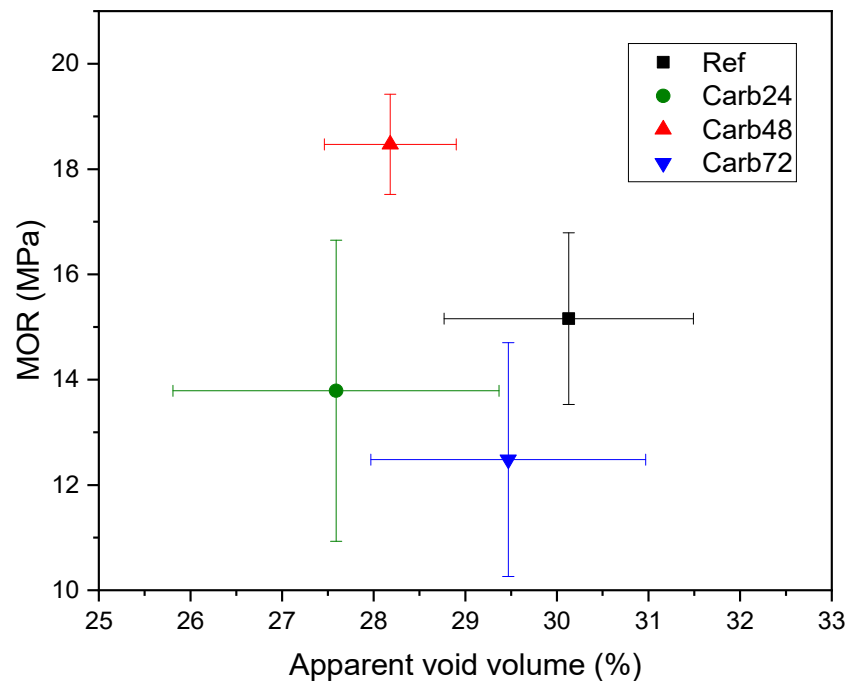


Figure 8. Mean values of modulus of rupture (MOR) vs. the apparent void volume of non-rehydrated composites. Horizontal and vertical lines indicate the standard deviation of each sample.

Figure 9 shows that the carbonation process with rehydration increased the mechanical strength of the boards and reduced the total void content of the composites for composites cured after 72 h (Carb72-RE). The increase in the mechanical performance of Carb72-RE boards is noteworthy, increasing 35.6% in MOR values and 35.5% in mean specific energy

values. By analyzing typical stress–strain curves, Carb48-RE and Carb72-RE composites exhibited the highest MOR values among the carbonated samples after rehydration. However, Carb72-RE samples showed higher deformation during mechanical loading, which aligns with their higher specific energy values at 4.08 KJ/m².

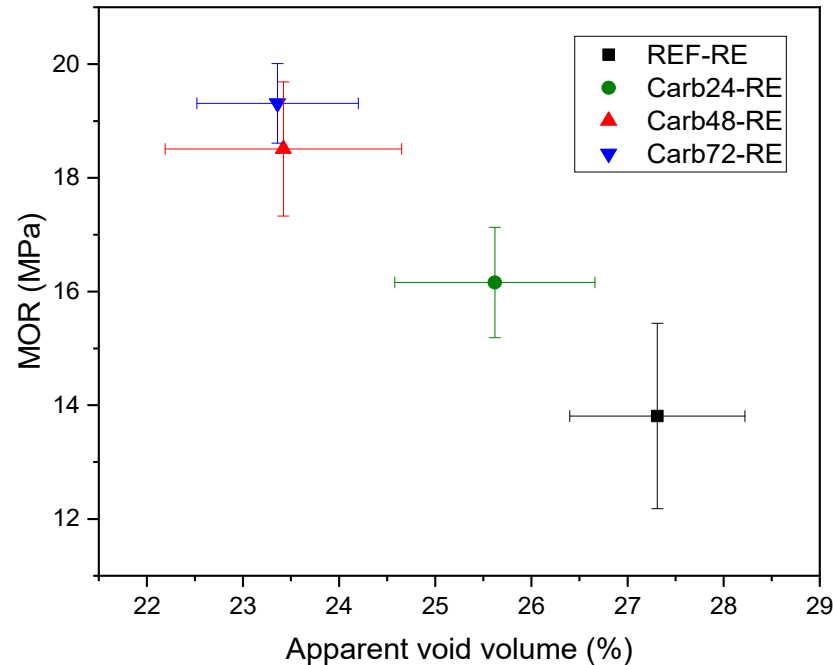


Figure 9. Mean values of modulus of rupture (MOR) vs. apparent void volume of rehydrated composites. Horizontal and vertical lines indicate the standard deviation of each sample.

An analysis of the comparison between the mean modulus of rupture (MOR) values and total void volume evidently shows that the accelerated carbonation process induces a trend towards reduced voids in the inorganic matrix, consequently enhancing the mechanical performance of the composites. The extent of this improvement varies depending on which pre-carbonation process is employed. The mean MOR values of Carb48 boards stand out compared with other boards cured for different periods. However, after the rehydration process, Carb48 RE and Carb72 RE boards exhibit higher mean MOR values, aligning with the observed trend of reduced voids following accelerated carbonation. Among the studied conditions, Carb72 RE boards demonstrate superior mechanical performance and a significant reduction in total voids. This improvement is attributed to the carbonation conditions induced by the prior curing process conducted in this investigation. The 72 h pre-curing process and the rehydration of the composites before accelerated carbonation facilitates the formation of carbonation products responsible for the observed mechanical changes, which are discussed in detail in the following sections.

3.2. Physical Properties

Tables 5 and 6 show the physical properties of carbonated cementitious composites. The accelerated carbonation process evidently led to changes in the mean values of water absorption, apparent porosity, and the apparent density of the carbonated materials (both rehydrated and non-rehydrated). The non-rehydrated Ref board showed higher mean water absorption value when compared with the carbonated one at different pre-cure times and after the rehydration of the boards. The decrease in water absorption by the carbonated boards after rehydration was associated with the improved carbonation process of the rehydrated materials, which promoted the formation of new carbonation products in the existing voids of the composites. The formation of carbonation products was favored by an extended pre-cure period and the rehydration of the boards before curing in a CO₂-rich

environment. The apparent density of the boards is indicative of carbonate formation during accelerated carbonation. The rehydration process of the boards before accelerated carbonation favored an increase in the mean density values. An increase of approximately 8.2, 4.3, 5.2, and 8.0% in the mean apparent density values was observed for the Ref-RE, Carb24-Re, Carb48-RE, and Carb72-RE samples, respectively. The similar density increase observed in the reference and Carb72-RE samples was associated with the formation of more $Mg(OH)_2$ in the samples after the rehydration process. However, the gain in mechanical strength of the Ref-RE boards was not comparable to the values obtained in the Carb48-RE and Carb72-RE boards, with the density increase related to the formation of carbonate products that enhance the mechanical performance of the composites.

Table 5. Physical proprieties of non-rehydrated-carbonated MOS-based fiber cement boards.

Sample	Water Absorption (%)	Apparent Porosity (%)	Bulk Density (g/cm^3)
Ref	19.98 ± 1.48	30.13 ± 0.76	1.46 ± 0.01
Carb24	18.08 ± 1.76	27.59 ± 0.78	1.53 ± 0.05
Carb48	19.09 ± 1.87	28.18 ± 1.03	1.52 ± 0.05
Carb72	19.38 ± 1.40	29.47 ± 1.13	1.50 ± 0.05

Table 6. Physical proprieties of rehydrated-carbonated MOS-based fiber cement boards.

Sample	Water Absorption (%)	Apparent Porosity (%)	Bulk Density (g/cm^3)
Ref-RE	17.21 ± 0.93	27.31 ± 0.91	1.59 ± 0.91
Carb24-RE	16.03 ± 1.10	25.62 ± 1.04	1.601 ± 0.045
Carb48-RE	14.63 ± 1.10	23.42 ± 0.93	1.603 ± 0.056
Carb72-RE	14.34 ± 0.78	23.36 ± 0.84	1.631 ± 0.033

3.3. Thermogravimetric Analysis (TGA/DTG)

Figure 10 shows the thermogravimetric analysis of carbonated (rehydrated and non-rehydrated) MOS matrix fiber cement samples. The analyzed materials exhibited similar behavior regarding thermal decomposition. Figure 11 shows that these composites display four distinct thermal events at similar temperatures. The temperature range of 90–200 °C shows the mass loss attributed to the decomposition of water molecules physically adsorbed on the surface and the commencement of decomposition of water molecules within the crystalline lattice of the 5-1-7 phase. This phase is primarily responsible for the enhancement of mechanical strength in MOS-type cement.

Figure 11 shows a second thermal event occurring at temperatures near 300–370 °C associated with the decomposition of lignocellulosic material used as a reinforcement in the produced composites. The most significant mass loss was observed within the temperature range of 390–500 °C, linked to the decomposition of brucite crystals formed during MgO hydration. Notably, a more pronounced peak was observed in the sample labeled Ref-RE, which underwent rehydration but not carbonation. This observation can be attributed to an excess of water molecules in the rehydrated and non-carbonated boards since the accelerated carbonation process consumes water molecules for the formation of hydrated magnesium carbonates (Equation (2)). The Ref-RE boards exhibit a higher quantity of brucite due to the hydration reactions that occur after the rehydration of MgO crystals that are not entirely consumed.

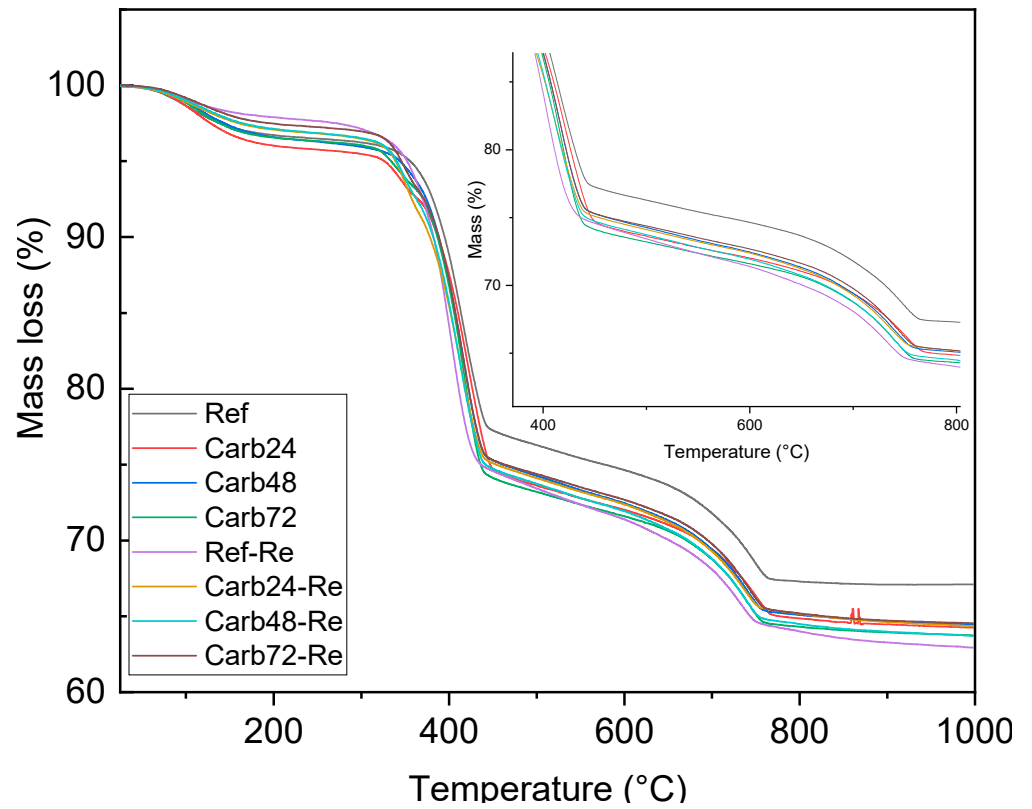


Figure 10. TGA analysis of rehydrated and non-rehydrated-carbonated MOS-based fiber cement boards.

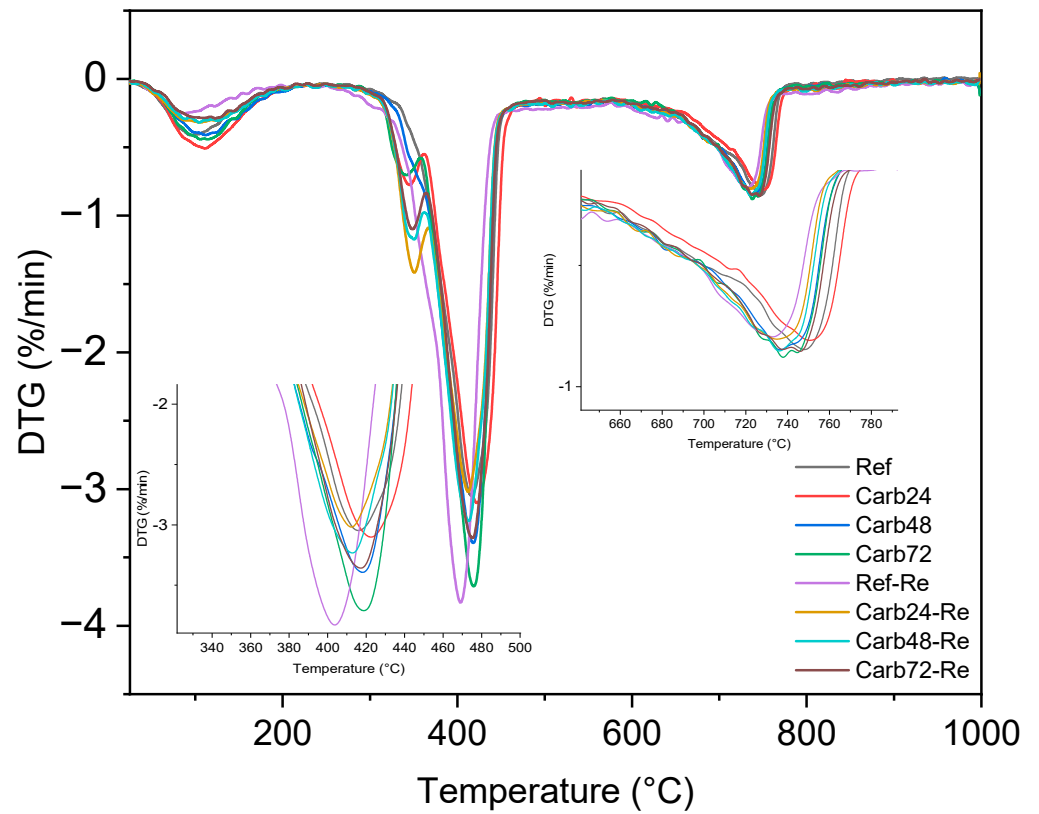


Figure 11. DTG analysis of rehydrated and non-rehydrated-carbonated MOS-based fiber cement boards.

The increased formation of $\text{Mg}(\text{OH})_2$ following the initiation of the curing process of the boards can be linked to the development of microcracks within the system due to expansion reactions during MgO hydration. This phenomenon can be connected to the reduced mechanical performance of the boards when compared with non-carbonated and non-rehydrated composites (Ref), resulting in an approximate 9.0% decrease in the mean MOR values of the boards. The carbonated samples under different pre-curing conditions exhibited similar mass losses. However, boards that rehydrated before curing in a CO_2 -rich atmosphere showed a decrease in the peak related to the decomposition of brucite. This could be attributed to the improved carbonation process of the boards by prior rehydration, facilitating the consumption of alkaline species for the formation of carbonates responsible for enhancing the mechanical properties of the studied composites.

The DTG analysis reveals that the rehydrated, non-carbonated board exhibited a decomposition band at temperatures close to 400°C associated with brucite. On the other hand, the carbonated boards (both rehydrated and non-rehydrated) presented a shift in this band to higher temperatures (420°C), linked to the formation of hydrated magnesium carbonates (HMC), as described in the work of Hay et al. (2020) [30]. These authors found that the carbonation process, in addition to altering the decomposition temperature of brucite, led to a greater loss of mass in the carbonated samples due to the decarbonization and increased dehydroxylation of these samples.

The mass loss observed in all samples in the temperature range from 650 to 790°C is associated with the decomposition of the limestone used as filler in the production of MOS cement boards.

3.4. Phase Analysis

Figure 12 shows the X-ray diffraction analyses of the crystalline phases formed during the production of both carbonated and non-carbonated MOS matrix fiber cement boards. Prominent peaks associated with the brucite phase (COD 96-100-0055), periclase (COD 96-900-6786), calcite (COD 96-900-9669), and crystalline phases linked to the 5-1-7 phase and responsible for the mechanical strength of the resulting boards are evident [20,23]. The rehydrated samples show an increase in the intensity of the diffraction peaks related to the brucite phase. In the Carb48-RE and Carb72-RE samples, the $\text{Mg}(\text{OH})_2$ phase peaks resemble those observed in the Ref sample (without carbonation), indicating that the rehydration process promotes new hydration products that facilitate carbonation. Rehydrated samples also exhibited a decrease in the intensity of the peaks associated with the periclase (MgO) phase, as observed at $43.0\ 2\theta$, which is related to the hydration of these MgO particles for the formation of brucite.

The 5-1-7 phase is present in the composites, which correlates with the demonstrated mechanical strength of these boards. However, the intensity of the diffraction peak, which closely aligned with the 5-1-7 phase at angles around $26.7^\circ\ 2\theta$, was reduced. This diffraction peak was also reduced in the carbonated samples after rehydration. This reduction in intensity could be associated with the formation of carbonation products with short-range atomic ordering (amorphous) on the surface of the boards, which interferes with the diffraction process of the other phases. This phenomenon may be linked to the decrease in the diffraction peaks of the calcite phases, a material used as a filler in the board formation, which exhibited reduced diffraction peaks in all samples after curing in a CO_2 -rich atmosphere (29.4 and $31.04\ 2\theta$).

3.5. SEM Analysis

Figure 13A–E show the analysis of the morphology of both carbonated and non-carbonated composites. The lignocellulosic materials are evidently embedded in the MgO -based matrix. These materials adhere to the inorganic matrix, and Figure 13A,B show fibers with a fractured appearance after mechanical loading. This phenomenon is related to the strong bond between the fiber and the matrix, facilitating the transfer of energy during the mechanical test and contributing to the increased specific energy of the

composites, as observed in the mechanical property results of the boards. Needle-shaped crystals (Figure 13C) related to the 5-1-7 phase were present in the materials under all conditions, demonstrating that the formulation used facilitated the formation of species responsible for the mechanical strength gain in the studied boards. Figure 13D shows the morphology of the Carb72 samples, which were not subjected to prior rehydration. The presence of brucite ($\text{Mg}(\text{OH})_2$) crystals on the surface of the samples is identifiable. This could be associated with the extended period before curing in a CO_2 -enriched environment. However, microcracks are noticeable, which could be linked to the expansive processes during MgO hydration. These microdefects may be associated with the reduction in mechanical strength observed in these samples and the increase in the mean values of water absorption and porosity.

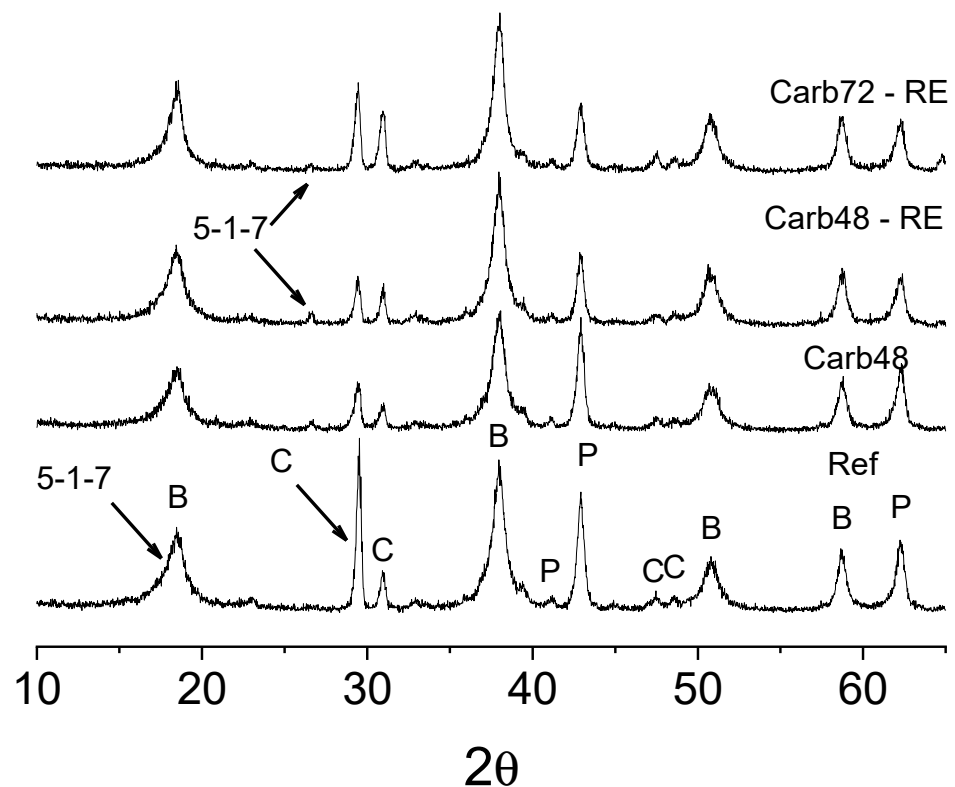


Figure 12. Diffraction patterns of rehydrated and non-rehydrated-carbonated MOS-based fiber cement boards. C—Calcite (CaCO_3), B—Brucite ($\text{Mg}(\text{OH})_2$) and P—Periclase (MgO).

Rehydrating the samples before the accelerated carbonation alters the physical–mechanical properties of the composites and is associated with the formation of new compounds. The presence of hydromagnesite ($4\text{MgCO}_3 \cdot \text{Mg}(\text{OH})_2 \cdot 4\text{H}_2\text{O}$) and brucite in the Carb72-RE samples is notable (Figure 13E). The appearance of this compound in relation to the carbonation process aligns with the findings of Unluer et al. [30], where the authors demonstrated that hydromagnesite crystals can form in environments containing $\text{Mg}(\text{OH})_2$, CO_2 , and additional water, correlating with the rehydrated boards after 48 and 72 h. The extended pre-curing period (48 and 72 h) is linked to the increased hydration of the MgO crystals and formation of $\text{Mg}(\text{OH})_2$ (Figure 13F), which promotes the formation of $4\text{MgCO}_3 \cdot \text{Mg}(\text{OH})_2 \cdot 4\text{H}_2\text{O}$ after carbonation and results in observed alterations in the physical–mechanical properties of the carbonated composites [31].

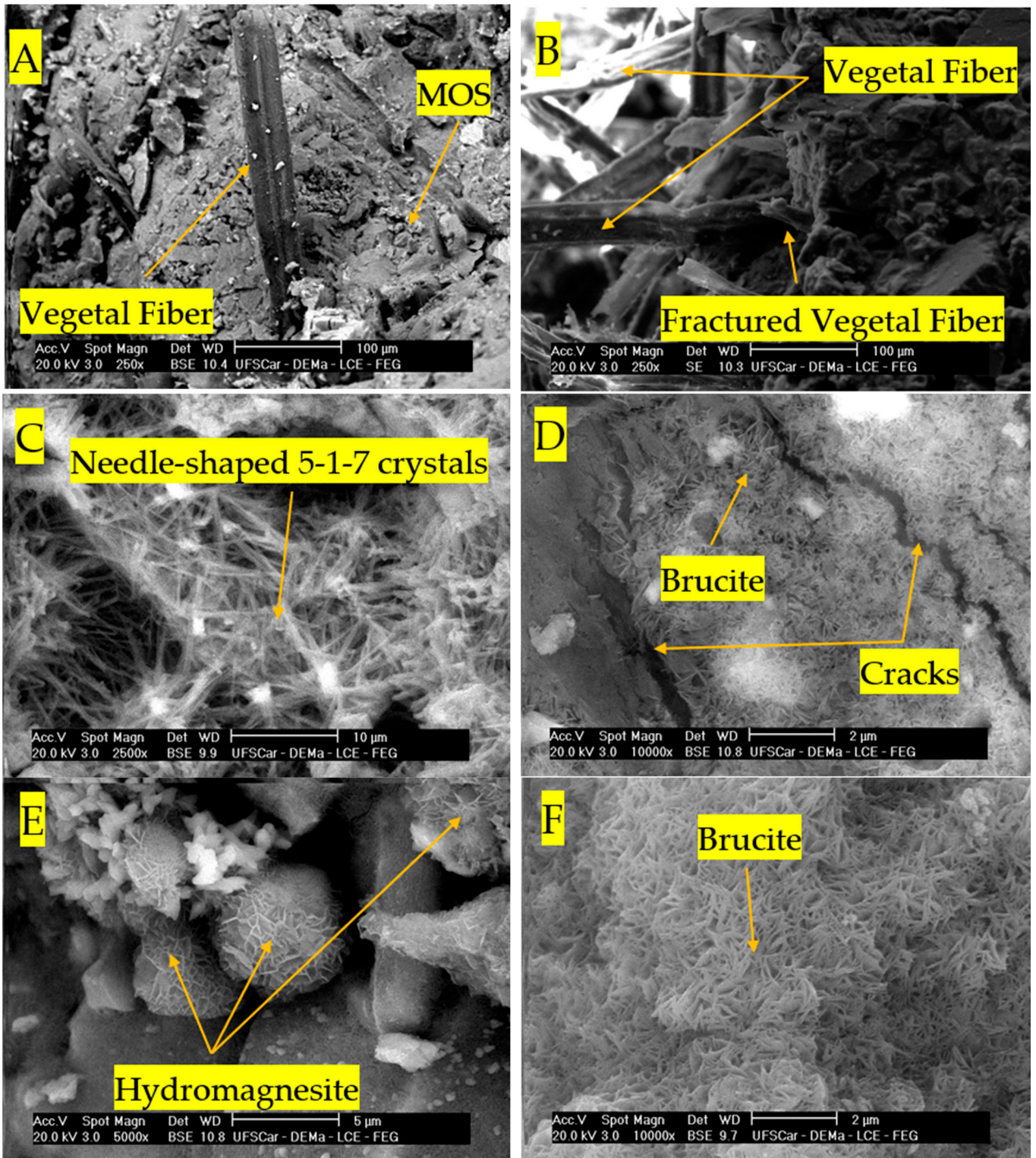


Figure 13. SEM images of rehydrated and non-rehydrated-carbonated MOS-based fiber cement: (A) Ref, (B) Carb48, (C) Carb48, (D) Carb72, (E) Carb72-RE, and (F) Carb72-RE.

4. Discussion

The production of MOS matrix fiber cement board serves as an alternative for mitigating the release of pollutants during the production of cementitious composites with common Portland cement matrices. The use of lignocellulosic fibers provides an alternative to asbestos and enhances the mechanical performance of the boards. The accelerated car-

bonation process employed in this study was an effective curing method for improving the final properties of composites produced with MOS matrices. It is essential to control the duration before exposure to a CO₂-enriched atmosphere with the provision of extra water before carbonated curing with board rehydration. The accelerated carbonation of MOS cement is achieved via the brucite reaction—the main product of MgO hydration—with CO₂. Carbonated materials exhibited increased mean values of the modulus of rupture (MOR) and modulus of elasticity (MOE) due to the formation of carbonation products. Carbonation reactions occur within the voids and pores of the matrices, promoting matrix stiffening, which results in reduced water absorption and apparent porosity values. Carbonation improved when board rehydration was applied before exposure to a CO₂-rich atmosphere. Longer periods before carbonation and prior rehydration favored the enhancement of the mechanical strength of the boards, with Carb48-RE and Carb72-RE samples showing the highest mean MOR values among the composites studied. Rehydration facilitated the formation of hydromagnesite crystals, which were observed in environments with high concentrations of Mg(OH)₂, CO₂, and H₂O and could be associated with the reduction in the intensity of diffraction peaks related to brucite, as observed in carbonated boards with prior rehydration. The use of accelerated carbonation led to more significant changes in the properties of non-rehydrated boards cured after 48 h and rehydrated ones cured after 48 and 72 h. The rehydration process can be applied to these boards to increase the water content in the system, yielding more hydration products, facilitating CO₂ dissolution, and the subsequent carbonation of MOS cement-based boards. Rehydrating MOS matrix fiber cement boards before carbonation can be an alternative due to the water loss caused by the Hatschek process simulation. This procedure, in addition to generating more hydration products, enhances the composite mechanical performance, which may be of interest to the fiber cement board market.

5. Conclusions

By analyzing the results related to the production and carbonation of MOS matrix fiber cement boards, the following can be concluded:

- The production of boards using the Hatschek process simulation was successful, and the composites presented satisfactory mechanical behavior after different types of curing were applied.
- The accelerated carbonation process of the boards resulted in more significant improvements in the rehydrated composites with the formation of hydromagnesite after curing in a CO₂-rich environment.
- The improvement of the mechanical performance of the boards was associated with the formation of new carbonation products, preferentially in the void space of the matrix. These new carbonation product formations were confirmed using TGA and SEM analysis.
- The pre-curing applied before carbonation proved to be a crucial step to control to obtain boards without microcracks and enhanced mechanical properties.
- The use of MOS cement in the production of fiber cement boards can be an alternative to the traditionally employed inorganic binders since they exhibit superior mechanical properties that can be further enhanced by subjecting the materials to accelerated carbonation.

Future efforts should focus on optimizing the production process, exploring alternative curing methods, and assessing the scalability and economic feasibility of large-scale MOS cement-based board production. Continued research on long-term durability, partnerships with industry stakeholders, and diverse applications emphasize MOS cement's potential to transform construction materials with enhanced mechanical properties and environmental benefits.

Author Contributions: Conceptualization, A.G.S.A., J.C.A.M., I.P. and T.O.G.F.; methodology, A.G.S.A., J.C.A.M., I.P. and T.O.G.F.; validation, A.G.S.A.; formal analysis, A.G.S.A.; investigation, A.G.S.A., J.C.A.M. and T.O.G.F.; resources, H.S.J., P.F. and A.C.; data curation, A.G.S.A.; writing—original draft preparation, A.G.S.A., J.C.A.M., I.P. and T.O.G.F.; writing—review and editing, A.G.S.A., J.C.A.M., I.P., T.O.G.F. and P.F.; visualization, A.G.S.A., P.F., A.C. and H.S.J.; supervision, H.S.J., P.F. and A.C.; project administration, H.S.J., P.F. and A.C.; funding acquisition, H.S.J., P.F. and A.C. All authors have read and agreed to the published version of the manuscript.

Funding: The São Paulo Research Foundation (FAPESP)—Processes: 2021/04780-7, 2022/07179-5, and 2014/50948-3. The CNPQ—Processes: 422701/2021-1 and 402980/2022-0. The Portuguese Foundation for Science and Technology (FCT) by funding CERIS research unit (UIDB/04625/2020) and the University of Minho.

Institutional Review Board Statement: Not applicable.

Informed Consent Statement: Not applicable.

Data Availability Statement: The data are contained within this article.

Conflicts of Interest: The authors declare no conflicts of interest.

References

1. Benhelal, E.; Zahedi, G.; Shamsaei, E.; Bahadori, A. Global strategies and potentials to curb CO₂ emissions in cement industry. *J. Clean. Prod.* **2013**, *51*, 142–161. [[CrossRef](#)]
2. Juenger, M.C.G.; Winnefeld, F.; Provis, J.L.; Ideker, J.H. Advances in alternative cementitious binders. *Cem. Concr. Res.* **2011**, *41*, 1232–1243. [[CrossRef](#)]
3. He, Z.; Zhu, X.; Wang, J.; Mu, M.; Wang, Y. Comparison of CO₂ emissions from OPC and recycled cement production. *Constr. Build. Mater.* **2019**, *211*, 965–973. [[CrossRef](#)]
4. Chen, C.; Habert, G.; Bouzidi, Y.; Jullien, A. Environmental impact of cement production: Detail of the different processes and cement plant variability evaluation. *J. Clean. Prod.* **2010**, *18*, 478–485. [[CrossRef](#)]
5. Maddalena, R.; Roberts, J.J.; Hamilton, A. Can Portland cement be replaced by low-carbon alternative materials? A study on the thermal properties and carbon emissions of innovative cements. *J. Clean. Prod.* **2018**, *186*, 933–942. [[CrossRef](#)]
6. Meng, D.; Unluer, C.; Yang, E.H.; Qian, S. Recent advances in magnesium-based materials: CO₂ sequestration and utilization, mechanical properties and environmental impact. *Cem. Concr. Compos.* **2023**, *138*, 104983. [[CrossRef](#)]
7. Wang, Y.; Wei, L.; Yu, J.; Yu, K. Mechanical properties of high ductile magnesium oxychloride cement-based composites after water soaking. *Cem. Concr. Compos.* **2019**, *97*, 248–258. [[CrossRef](#)]
8. Ruan, S.; Unluer, C. Comparative life cycle assessment of reactive MgO and Portland cement production. *J. Clean. Prod.* **2016**, *137*, 258–273. [[CrossRef](#)]
9. Liska, M.; Al-Tabbaa, A.; Carter, K.; Fifield, J. Scaled-up commercial production of reactive magnesium cement pressed masonry units. Part I: Production. *Proc. Inst. Civ. Eng. Constr. Mater.* **2012**, *165*, 211–223. [[CrossRef](#)]
10. Shand, M.A. *The Chemistry and Technology of Magnesia*; Wiley-Interscience: Hoboken, NJ, USA, 2006.
11. Nobre, J.; Ahmed, H.; Bravo, M.; Evangelista, L.; De Brito, J. Magnesia (Mgo) production and characterization, and its influence on the performance of cementitious materials: A review. *Materials* **2020**, *13*, 4752. [[CrossRef](#)]
12. Walling, S.A.; Provis, J.L. Magnesia-Based Cements: A Journey of 150 Years, and Cements for the Future? *Chem. Rev.* **2016**, *116*, 4170–4204. [[CrossRef](#)] [[PubMed](#)]
13. Schorcht, F.; Kourti, I.; Scalet, B.M.; Roudier, S.; Sancho, L.D. *European Commission, Joint Research Centre (IEC JRC), European Integrated Pollution Prevention and Control Bureau (EIPPCB). Best Available Techniques (BAT) Reference Document for the Production of Cement, Lime and Magnesium Oxide*; Publications Office of the European Union: Luxembourg, 2013.
14. Shand, M.A. Magnesium oxysulfate cement. *Magnes. Cem.* **2020**, *1*, 75–83. [[CrossRef](#)]
15. Chen, F. Study on preparation and properties of modified magnesium oxysulfate cements. *Chem. Eng. Trans.* **2017**, *62*, 973–978. [[CrossRef](#)]
16. Ba, M.; Xue, T.; He, Z.; Wang, H.; Liu, J. Carbonation of magnesium oxysulfate cement and its influence on mechanical performance. *Constr. Build. Mater.* **2019**, *223*, 1030–1037. [[CrossRef](#)]
17. Gu, K.; Chen, B.; Yu, H.; Zhang, N.; Bi, W.; Guan, Y. Characterization of magnesium-calcium oxysulfate cement prepared by replacing MgSO₄ in magnesium oxysulfate cement with untreated desulfurization gypsum. *Cem. Concr. Compos.* **2021**, *121*, 104091. [[CrossRef](#)]
18. Hao, Y.; Li, C.; Zhao, F. Study on water resistance modification of magnesium oxysulfate cement. *IOP Conf. Ser. Mater. Sci. Eng.* **2019**, *493*, 012079. [[CrossRef](#)]
19. Demediuk, T.; Cole, W.F. A study on magnesium oxysulphates. *Aust. J. Chem.* **1957**, *10*, 287–294. [[CrossRef](#)]
20. Grünhäuser Soares, E.; Castro-Gomes, J. Carbonation curing influencing factors of Carbonated Reactive Magnesia Cements (CRMC)—A review. *J. Clean. Prod.* **2021**, *305*, 127210. [[CrossRef](#)]

21. Mármol, G.; Savastano, H. Study of the degradation of non-conventional MgO-SiO₂ cement reinforced with lignocellulosic fibers. *Cem. Concr. Compos.* **2017**, *80*, 258–267. [[CrossRef](#)]
22. Dung, N.T.; Lesimple, A.; Hay, R.; Celik, K.; Unluer, C. Formation of carbonate phases and their effect on the performance of reactive MgO cement formulations. *Cem. Concr. Res.* **2019**, *125*, 105894. [[CrossRef](#)]
23. Sun, Q.; Ba, M.; Zhang, D.; Zhou, S.; Zhang, N.; Wang, F. Effects of citrate acid, solidum silicate and their compound on the properties of magnesium oxysulfate cement under carbonation condition. *Constr. Build. Mater.* **2022**, *330*, 127136. [[CrossRef](#)]
24. Li, Q.; Su, A.; Gao, X. Preparation of durable magnesium oxysulfate cement with the incorporation of mineral admixtures and sequestration of carbon dioxide. *Sci. Total Environ.* **2022**, *809*, 152127. [[CrossRef](#)] [[PubMed](#)]
25. TAPPI T 271 om-23, "Fiber length of pulp and paper by automated optical analyzer using polarized light" (Technical Association of the Pulp & Paper Industry, 2023). Available online: <https://imisrise.tappi.org/TAPPI/Products/01/T/0104T271.aspx> (accessed on 28 October 2023).
26. Van Soest, P.J. *Nutritional Ecology of the Ruminant*; Cornell University Press: New York, NY, USA, 2018.
27. Savastano, H.; Warden, P.G.; Coutts, R.S.P. Brazilian waste fibres as reinforcement for cement-based composites. *Cem. Concr. Compos.* **2000**, *22*, 379–384. [[CrossRef](#)]
28. ASTM C 948-81; ASTM C 948-81 (Reapproved 2016) Standard Test Method for Dry and Wet Bulk Density, Water Absorption, and Apparent Porosity of Thin Sections of Glass-Fiber REINFORCED Concrete. ASTM-American Society for Testing Materials: West Conshohocken, PA, USA, 2016; Volume 81, pp. 1–2.
29. RILEM Reunion Internationale des Laboratoiores d'essais et des Recheches sur les Materiaux et les Constructions. RILEM Technical Committee 49TFR: Testing methods for fibre reinforced cement-based composites. *Mater. Constr.* **1984**, *17*, 441–456.
30. Hay, R.; Celik, K. Hydration, carbonation, strength development and corrosion resistance of reactive MgO cement-based composites. *Cem. Concr. Res.* **2020**, *128*, 105941. [[CrossRef](#)]
31. Unluer, C.; Al-Tabbaa, A. Green Construction with carbonating reactive magnesia porous blocks: Effect of cement and water contents. In Proceedings of the International Conference on Future Concrete, Dubai, United Arab Emirates, 12–14 December 2011.

Disclaimer/Publisher's Note: The statements, opinions and data contained in all publications are solely those of the individual author(s) and contributor(s) and not of MDPI and/or the editor(s). MDPI and/or the editor(s) disclaim responsibility for any injury to people or property resulting from any ideas, methods, instructions or products referred to in the content.